G-Mode KPFM: Bringing Kelvin probe into the information age

L. Collins*, S. V. Kalinin and S. Jesse

Institute for Functional Imaging of Materials & Center for Nanophase Materials Sciences, Oak Ridge National Laboratory, Oak Ridge, Tennessee 37831, USA

ABSTRACT

Kelvin probe force microscopy (KPFM) has provided deep insights into the local electronic, ionic and electrochemical functionalities in a broad range of materials and devices. However, the technique is known to suffer from artifacts associated with non-ideality of bias feedback as well as being unsuitable for some voltage sensitive materials. Furthermore, in many applications, it is dynamic electrochemical processes which determine overall functionality, whereas KPFM can only measure static or quasistatic properties. Here we describe General acquistion (G)-Mode KPFM, which works by streaming the excitation signal and the photodetector signal straight to computer memory, bypassing the AFM controllers many filters and demodulation pathways. In this work, we outline a set of protocols for (a) denoizing (b) visualising and (c) quantifying the multidimensional datasets while preserving the temporal information on the tip-sample interactions. We investigate the veracity of the G-Mode KPFM approach for quantification of surface potential in two different ways. First we compare the single point surface potential values measured using G-Mode KPFM on a gold electrode whose surface potential is modulated with a known voltage. Afterwards we directly compare G-Mode KPFM imaging capabilities with conventional KPFM on a model test sample. In the future, G-KPFM while provide a real oppurtunity to explore dynamic processes taking place between tip and sample which is key towards developing a complete understanding of functionality in a range of systems including battery materials, photovoltaics and biosystems.

Keywords: Kelvin probe force microscopy, atomic force microscopy, surface potential, big data.

1 BACKGROUND

Fundamental mechanisms of energy storage,[1] corrosion,[2] sensing,[3] and multiple biological functionalities[4] are directly coupled to electrical processes and ionic dynamics at both the solid-gas and solid-liquid interfaces. In many cases, these processes are spatially inhomogeneous (e.g., grain boundaries, step edges, point defects, ion channels), and possess complex time and voltage dependent dynamics.

Kelvin probe force microscopy (KPFM),[5] which combines the age old Kelvin method with the atomic force microscope (AFM),[6] has provided deep insights into the local electronic, ionic and electrochemical functionalities in a broad range of energy materials, biosystems and devices. Despite the popularity of KPFM,[7] the technique is known to suffer from inherent artifacts which can lead to systematic errors in absolute values recorded,[8,9] making comparison between experiments or with modelling difficult. Furthermore, the level of information available is not sufficient for some electroactive systems, or operation in liquid electrolytes, involving time and bias dependent electrochemical phenomena.[10,11] Practically, this limitation stems from the detection methodologies adopted in classical KPFM, and AFM in general, which limit the time resolution of the measurement and mask any underlying fast processes. In this work, General Acquisition mode[12] (G-Mode) KPFM will be described. We demonstrate quantitative KPFM measurements using this approach while overcoming many of the drawbacks of conventional KPFM (e.g. bias feedback, slow readout rates). In this work we outline a set of protocols for (a) denoizing (b) visualising and (c) quantifying the multidimensional datasets afforded by G-Mode KPFM.

2 EXPERIMENTAL

2.1 Kelvin Probe Force Microscopy

In KPFM the cantilever is scanned at a predefined distance above the sample (typically 50-200 nm) as the tip is biased directly by $V_{tip} = V_{dc}+V_{ac}\cos(\omega t)$, where V_{ac} is referred to as the driving voltage. The capacitive force, $F_{cap}(z)$, between the tip and a surface having a built in electrostatic or "contact" potential difference (CPD) V_{CPD} is:

$$F_{cap}(z)=\frac{1}{2}\left(V_{tip}-V_{CPD}\right)^2\frac{\partial C(z)}{\partial z} \quad \textbf{[1]}$$

where $C(z)$ is the tip-surface capacitance dependent on tip geometry, surface topography and tip surface separation, z. Since V_{tip} is time dependent, the force has spectral components comprising a static DC capacitive force, as well as forces at the modulation frequency (ω, the first harmonic), and forces at double of the frequency of the tip voltage (2ω, the second harmonic), as described by Equations 2-4.

$$F_{DC}^{cap}(z)=-\frac{\partial C(z)}{\partial z}\left(\frac{1}{2}(V_{dc}-V_{CPD})^2+\frac{1}{4}{V_{ac}}^2\right) \quad \textbf{[2]}$$

$$F_{1\omega}^{cap}(z)=\frac{\partial C(z)}{\partial z}\left(V_{dc}-V_{CPD}\right)V_{ac}\sin(\omega t) \quad \textbf{[3]}$$

$$F_{2\omega}^{cap}(z)=\frac{1}{4}\frac{\partial C(z)}{\partial z}V_{ac}^2\cos(\omega t) \quad \textbf{[4]}$$

In amplitude modulated KPFM a lock in amplifier (LIA) is typically used to detect the first harmonic response, attenuating all other information regarding the tip-sample interactions outside of this frequency. The excitation frequency is maintained constant during imaging, and the amplitude and phase information is extracted as the output of the LIA. Bias feedback is used to nullify this term (Equation 3) by adjusting

the tip bias, V_{dc}. This condition is met when V_{dc} is equal to CPD and thus, mapping the nulling potential V_{dc} yields a CPD map. Under the condition of $F_{1\omega}^{cap} = 0$, the measured CPD can then be determined independently from measurement parameters. In practice, however, the interpretation of the recorded CPD requires careful consideration of the influence of the instrumentation, and in particular the bias feedback loop.[7, 8]

2.3 Materials

Measurements were performed using Asylum Research, Cypher system and as-received Pt/Ir conductive probes (*Multi 75-G, BudgetSensors*) having a nominal mechanical resonant frequency and spring constant of ~75 kHz and ~2.8 N/m, respectively. The samples were mounted on 15 mm steel pucks (Ted Pella) using conductive silver paint (Agar Scientific Ltd.) as ground path with respect to the tip. Measurements were performed on the interface of a model system containing a Silicon- Gold (40 nm) interface at a tip-sample distance of 100 nm. The substrate is assumed to have a native oxide (i.e. SiO_x) and local modification of the SiO_x was realized using a bias tip (20 V) scanned in contact over a 3 μm^2 region.

2.2 General Acquisition mode

At their core, traditional KPFM techniques rely on heterodyne detection, which has the effect of limiting both the information captured (i.e. attenuation of all response outside detection frequency) as well as imposing bandwidth limitations (i.e. LIA time constant). In 2015, general acquisition mode (G-Mode) SPM was developed,[7] allowing full exploration of the cantilever deflection with extremely high temporal resolution. In the short time since its inception, the G-Mode approach has been shown to have advantages for tapping mode AFM,[7] PFM,[13] MFM[14] and KPFM.[15, 16] The approach overcomes the drawbacks of existing AFM techniques by capturing and storing cantilever dynamics at high speed over a broad range of frequencies, ultimately trading heterodyne detection and closed loop feedback for large multidimensional data sets. The G-Mode measurements shown in this work were implemented using a LabView/Matlab controller implemented in PXI architecture using National Instruments NI-6124 fast AWG and DAQ cards and is readily implementable on all SPM platforms

3 RESULTS

3.1 Bias spectroscopy

To check the veracity of G-Mode KPFM we perform a measurement with the tip held stationary above a gold electrode while a linear DC bias waveform (-3 to 3V) is supplied to the electrode. An AC voltage (4 V_{peak} at 20 kHz) is applied to the tip, while the response of the cantilever, which is encoded in the photodetector signal, is streamed (at 4 MHz sampling rate) directly to the computer hardrive for post processing analysis. The stored data is then processed and analyzed in a variety of fashions. The first approach is to emulate heterodyne detection normally used in AFM.[15] We do this in digital space by calculating the ratio of the Fast fourier transform (FFT) of the response, at a given frequency, to the FFT of the input signal at the drive frequency. The output is an amplitude and phase response similar to conventional LIA. Clearly, an obvious advantage to performing this operation digitally is the ability to inspect the cantilever response at each frequency separately. In comparison to traditional AFM, we can do so without having to repeat the experiment with a different LIA setting or using multiple LIA channels.

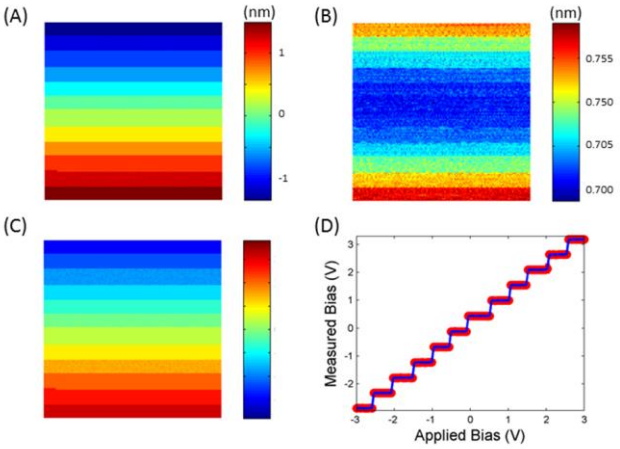

Figure 1. (a) First and (b) second harmonic in phase response to the electrostatic force recorded as a function of surface voltage (-3V to 3V, top-bottom). (c) Recovered surface potential determined using Equation 5, V_{ac}= 4 and X_{gain}= 0.805. (d) Measured surface potential plotted versus appled surface voltage.

In Figure 1(a, b) the first and second harmonic amplitude response is shown. In Figure 1(a) the in-phase component is shown (i.e. $A_\omega\cos(\varphi_\omega)$ where φ_ω is phase) as the phase determines the polarity of the CPD. The second harmonic response is not sensitive to the surface voltage and the observed changes, at large voltage magnitudes (see Figure 1(b)), are indicitive of small changes in the tip to sample distance as a result of tip deflection. Since the first harmonic response contains information on the V_{CPD}, and the second harmonic contains purely capacitance response, the ratio of the harmonics can be used to determine V_{CPD} as described by Equation 5;

$$V_{CPD} = \frac{A_\omega \cos(\varphi_\omega)}{A_{2\omega}} \frac{V_{ac}}{4X_{gain}} \quad \textbf{[5]}$$

for a given V_{ac} and with knowledge of cantilever transfer function gain, X_{gain}.[15] The heterodyne analogue of this approach is known as Dual Harmonic (DH)-KPFM, first developed for application towards voltage sensitive materials, and later adapted to studies of the solid-liquid interface.[17] Figure 1(c) and (d) show the calculated V_{cpd} which was found to track the applied voltage precisely having a 6V range corresponding to the applied surface bias modulation plus a offset of 119 ± 8 mV corresponding to the CPD.

3.2 Unbiased analysis methods

One problem with the heterodyne approach above is that the response needs to be averaged over a long integration time (typically pixel time ~1-4ms) to enable sufficient noise reduction. Ultimately this leads to a single read-out of amplitude and phase, and hence V_{CPD}, for each pixel. It is this methodology that limits KPFM measurement to stationary or slow electrochemical processes. In addtion, for extremely non-linear processes (e.g. transient charging) or in the presence of liquids (e.g. response is not purely electrostatic) the energy of cantilever may not be confined to 2 harmonics alone and additional higher harmonics (or intermodulation products) may be present in the cantilever response spectrum. Therefore, we explore multivariate statistical approaches for detection of relevant cantilever dynamics without priori knowledge on imaging mechanism or on the system parameters.

Principal component analysis (PCA) is a fast method to analyze multidimensional datasets as well as a useful tool for denoizing such data sets. It works by perfroming a principal axis rotation of the variance–covariance matrix of the original dataset and converts it into a linear superposition of orthogonal, linearly uncorrelated eigenvectors. The direction cosines between the new and old axes are eigenvectors calculated by the singular value decomposition of the variance–covariance matrix, C = AAT where A is the matrix of all experimental data points Aij, i.e., the rows of A correspond to individual grid points i = 1, . . n. and columns correspond to voltage points, j = 1,. . . .n. The resulting variables, or principal components (PC), are orthogonal and as such uncorrelated, and are arranged such that corresponding eigenvalues loading maps are placed in descending order, by variance.

Figure 2 shows the outcome of PCA of data described in Figure 1. In this case, all of the temporal information (since the tip is held stationary in position) in the loading maps is confined to the first 3 PC (see Figure 2(a)-(c)) and all subsequent PC are featureless (not shown). Inspection of the PC eigenvectors can be used to map these loading maps directly onto physical interactions. In Figure 2(d-f) the full eigenvector responses are plotted against the applied tip voltage (color scale indicates pixel time). Clearly, both the first and the third PC have squared voltage dependence whereas the second PC respone has a linear voltage dependence. From equations [2]-[4] we expect the DC and 2ω component to be dependent on the square of the voltage whereas the first harmonic response has a linear bias dependence. Comparing the loading map of PC2 with Figure 1(b) it is clear that PCA can isolate the response detected using LIA, but also preserves the time component as seen in the corresponding eigenvector. The fact the the DC component is much larger thant the second harmonic response (i.e. the static deflection of the cantilever is what drives the contrast seen in Figure 2(b)) we can speculate that the DC component dominates PC1 and the second harmonic component is the main contribution to PC3. In this case, since the surface bias is constant over the pixel time the eigenvectors demonstrate statio-temporal behaviour, however we expect that fast transient events can be revealed in dispersion of the time dependent eigenvectors.

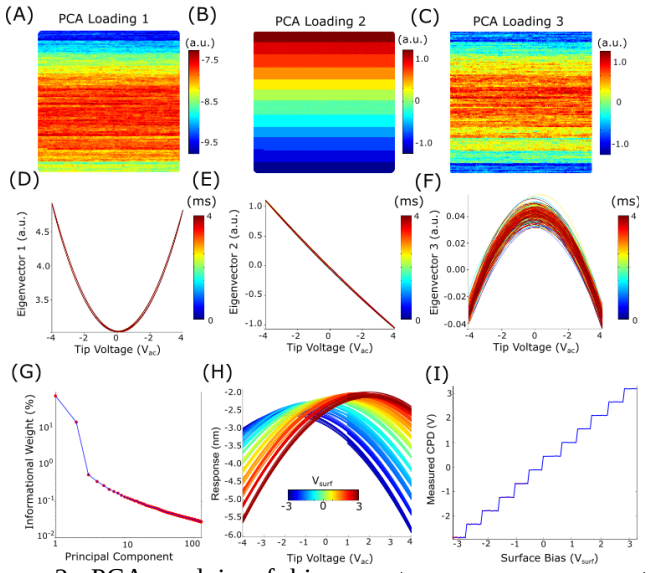

Figure 2. PCA analyis of bias spectroscopy measurement showing the first three principal components, showing the (a-c) Loading maps and (d-f) Eigenvectors where the colorscale shows the pixel response time. (g) The skree plot for the PC (h) recovered response as a function of tip voltage and (i) CPD determined from parabolic fitting of recovered response.

The skree plot, shown in Figure 2(g) can be used as a tool to determine how to reconstruct a denoized dataset without significant information loss. The skree basically describes the variance captured in each principal component. Here it is expressed as the fraction of the eigenvector divided by the sum of the eigenvalues for all the principal components in the model. Inspection of the skree plot reveals that the three PCs shown correspond to 97.42% of informational weight of the total dataset, and the subsequent PCs are dominated by noise. In this way, PCA allows the user to denoize the large (~4 Gb) multidimensional (X,Y,t) data set without trading temporal information. In Figure 2(h) the reconstructed signal is plotted as a function of tip voltage. The parabolic voltage dependence is expected from Equation 1, and fitting to a simply polynomial allows the CPD to be determined directly from tip voltage corresponding to the maxima of the parabola (note information on the capacitance can also be infered from the parabolic fit). In this case the time averaged CPD, determined from the mean CPD value of parabolic fitting to each AC oscillation, is shown in Figure 2(i). The values match precisely with the voltage applied to the surface and the CPD measured using the heterodyne approach (116 ± 6 mV).

3.3 Unbiased analysis methods

Figure 3 demonstrates the imaging capabilities of the G-Mode KPFM on an Au (40 nm) electrode on a Si surface with a small region (3 μm^2) which was locally charged using a biased tip (20 V) in contact with the surface. Figure 3(a) shows the

topography whereas (b) and (c) show the first and second order fit parameters from the parabolic fit which are related to capacitance gradinet and surface charge density respectively. Figure 3(d) shows the CPD measured using conventional KPFM where as Figure 4(d) shows the time averaged CPD obtained using G-Mode KPFM for comparison. Whereas Figure 3(f) is a cross section of the CPD measured over approximately the same area using both KPFM approaches. Signifanct deviation (~460 mV) in CPD were observed over the charged SiO_x region, which is expected due to slow compenstation of the charge by adsorbates in ambient within the time it took to perform both measurements. However, comparison of values on the gold electrode showed reasonable agreement although a 52 mV offset was detected between the techniques in agreement with previous studies comparing open and closed loop KPFM approaches and were assigned to non-ideality of the bias feedback loop.[9,15] Noteworthy, the G-KPFM data contains temporal information resulting in 202 read outs of CPD for every pixel shown, or a read out for every period of tip voltage oscillation (i.e. 50 µs). However, in this system, the CPD was found to be constant in time, in future the application to dynamic systems such as photvoltaic devices will be performed.

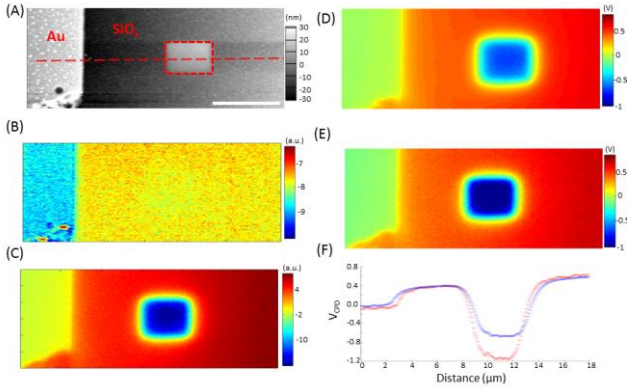

Figure 3. (a) Topography (scale bar = 5 µm) and G-KPFM (b) first and (c) second order polynomial fitting parameters. (d) CPD measured using (d) KPFM and (e) G-KPFM and cross sectional data (G-KPFM (red), KPFM (Blue)).

4 CONCLUSIONS

We have shown that it is possible to quantify the local electronic properties based on the reconstruction of bias dependence of a voltage modulated AFM probe, without the need for bias feedback or heterodyne detection. This is made possible using the G-Mode data collection platform combined with sophisiticated signal proccessing methods which do not require a priori model and preserve the temporal component of the response. We show that the time averaged CPD in G-Mode KPFM matches closely with that measured using standard KPFM. In future we believe the fast read out read of CPD permitted by the real time recovery of the electrostatic force will allow exploration of fast (<µs) electrodynamics making it a promising framework to improve our understanding of dynamic material functionalities such as ionic and charge transport as well as a promising approach for implementation of liquid KPFM.

5 ACKNOWLEDGEMENTS

Research was conducted at the Center for Nanophase Materials Sciences, which is sponsored at Oak Ridge National Laboratory by the Scientific User Facilities Division. This manuscript has been authored by UT-Battelle, LLC under Contract No. DE-AC05-00OR22725 with the U.S. Department of Energy. The United States Government retains and the publisher, by accepting the article for publication, acknowledges that the United States Government retains a non-exclusive, paid-up, irrevocable, world-wide license to publish or reproduce the published form of this manuscript, or allow others to do so, for United States Government purposes. The Department of Energy will provide public access to these results of federally sponsored research in accordance with the DOE Public Access Plan (http://energy.gov/downloads/doe-public-access-plan).

6 REFERENCES

1. S. V. Kalinin and N. Balke, Adv. Mat. **22** (35) (2010).
2. H. Böhni, T. Suter and A. Schreyer, Electrochim. Acta **40** (10), 1361-1368 (1995).
3. T. G. Drummond, M. G. Hill and J. K. Barton, Nat. Bio. **21** (10), 1192-1199 (2003).
4. R. Plonsey, *Bioelectric phenomena*. (Wiley Online Library, 1969).
5. M.Nonnenmacher,M.P.O'Boyle and H.K. Wickramasinghe, Appl. Phys. Lett. **58** (25), 2921 (1991).
6. G. Binnig, C. F. Quate and C. Gerber, Phys. Rev. Lett. **56** (9), 930-933 (1986).
7. L. Collins, J. Kilpatrick, S. V. Kalinin and B. J. Rodriguez, arXiv preprint arXiv:1701.06633 (2017).
8. S. Kalinin and D. Bonnell, Phys. Rev. B **63** (12), 125411 (2001).
9. L. Collins, et al., Nanotechnology **24** (47), 475702 (2013).
10. L. Collins, et al., Nat. Comm. **5** (2014).
11. L. Collins, S. Jesse, J. I. Kilpatrick, A. Tselev, M. B. Okatan, S. V. Kalinin and B. J. Rodriguez, Beil. J. Nano. **6** (1), 201-214 (2015).
12. A. Belianinov, S. V. Kalinin and S. Jesse, Nat. Comm. **6** (2015).
13. S. Somnath, A. Belianinov, S. V. Kalinin and S. Jesse, Appl. Phys. Lett. **107** (26), 263102 (2015).
14. L. Collins, et al, Appl. Phys. Lett. **108** (19), 193103 (2016).
15. L. Collins, et al., Nanotechnology **27** (10), 105706 (2016).
16. L. Collins, A. Belianinov, S. Somnath, N. Balke, S. V. Kalinin and S. Jesse, Scientific Reports **6** (2016).
17. L. Collins, et al., Appl. Phys. Lett. **104** (13), 133103 (2014).